Available online at www.sciencedirect.com
ScienceDirect
Thermochimica Acta 462 (2007) 64–69
thermochimica acta
www.elsevier.com/locate/tca

Electrical resistivity study and characterization during NiTi phase transformations

V. Antonucci *, G. Faiella, M. Giordano, F. Mennella, L. Nicolais

Institute for Composite and Biomedical Materials Technology CNR, P. le Tecchio 80, 80125 Napoli, Italy

Received 30 October 2006; received in revised form 28 May 2007; accepted 29 May 2007
Available online 9 June 2007

Abstract

In this study an experimental characterization of NiTi wires has been performed by calorimetric and electrical measurements. The evaluation of transition temperatures has been conducted by differential scanning calorimetry (DSC) analysis and electrical resistivity measurements. The latter method has been demonstrated to be a very useful technique for the identification of transition phases that are not detectable from calorimetric analysis. Moreover, calorimetric and electrical method have been used in order to quantify converted fractions of Martensite and R-phases as a function of temperature.

Keywords: Nitinol; Electrical resistivity; Transition

1. Introduction

Shape memory alloys exhibit some unique properties such as recovering macroscopic shapes previously imposed at a characteristic temperature or by particular loading cycles. Nitinol, a NiTi binary alloy, is the most commercially viable shape memory alloy because of its superior mechanical properties and chemical resistance.

The phenomenon related to the temperature effect is known as shape memory effect. This particular effect involves thermoelastic reversible crystallographic phase transformation from high-temperature phase (B2), named Austenite (A), to a low-temperature phase (monoclin), named Martensite (M) [1]. Another important effect showed by shape memory alloys is the pseudoelastic effect, based on a shape recovery by an unloading cycle at a particular temperature. This effect is related to a reversible microstructural deformation mechanism, known as stress induced transformation that generates a phase named stress induced Martensite.

In addition to Austenite and Martensite, in some special cases, an intermediate phase known as R-phase, having a trigonal crystal structure is present in the alloy during the cooling. The presence of R-phase is related to alloy's composition, thermal history and manufacturing. In these cases, the direct transformation is a two-stage process: Austenite phase at high-temperature transforms to intermediate R-phase and then to Martensite, the low-temperature phase.

The effect of heat treatment and thermal cycling on the various NiTi phases under stress free condition have been widely studied by Uchil et al. [2,3] which found that R-phase can form in a specified range of heat treatment temperatures depending on the particular alloy's composition.

The transformation behavior can be studied by different tools such as electrical resistivity [4–10], differential scanning calorimetry (DSC) [11,12], internal friction measurement [13], magnetic susceptibility [14,15], and thermoelectric power [16].

In particular, some authors [2,3,7–10] showed that electrical resistivity measurements can be a useful and good probe for the identification of both temperature and stress induced transformations involving SMA crystallographic phases. Uchil et al. [2] investigated 40% cold-worked Nitinol phase transformations as a function of heat treatment by measuring electrical resistivity variations with temperature, finding that electrical resistivity measurement is a very effective method for the understanding of shape memory transformations in NiTi under stress free condition. They observed that resistivity increases at Martensite → Austenite and decreases at Austenite → Martensite transformations. Moreover, if R-phase

* Corresponding author. Tel.: +39 0817758836; fax: +39 0817758850.
E-mail address: vinanton@unina.it (V. Antonucci).

0040-6031/$ – see front matter © 2007 Elsevier B.V. All rights reserved.
doi:10.1016/j.tca.2007.05.024

is present, resistivity approaches to a maximum value and during the cooling step, when resistivity increases, it is possible to evaluate R-phase start and finish temperatures.

In the present study, a thermal and electrical characterization of two different alloys $Ni_{55.4}Ti_{44.6}$ and $Ni_{54.8}Ti_{45.2}$ in form of wires has been performed. Transition temperatures have been determined by calorimetric measurements (DSC), that clearly revealed the presence of R-phase only in $Ni_{55.4}Ti_{44.6}$ alloy during the cooling step. Electrical resistance measurements have been carried out in order to study the transformation behavior and compare it with calorimetric results. Electrical resistance as function of temperature shows similar behavior for both the two alloys during the cooling: a rapid and large increase corresponding to the transformation from Austenite to R-phase. Moreover, the transformation degree of NiTi different phases during the whole thermal cycle (heating and cooling) has been evaluated both from DSC and resistivity data finding a good agreement between them. The comparison between calorimetric and electrical measurements pointes out the importance of temperature dependence of NiTi electrical resistance for the identification of particular transformation that otherwise could not be identifiable by calorimetric techniques.

2. Experimental

2.1. DSC analysis

Two different Nitinol alloys, $Ni_{55.4}Ti_{44.6}$ and $Ni_{54.8}Ti_{45.2}$ in form of wire of 0.5 mm and 0.38 mm diameter respectively, have been purchased by Memory-Metalle GMBH.

Calorimetric analysis has been performed by employing a DSC TA Instruments 2920 under dynamic conditions using a constant rate of heating and cooling of 10 °C/min. Heat-flow vs. temperature curves are shown in Figs. 1 and 2 for $Ni_{55.4}Ti_{44.6}$ and $Ni_{54.8}Ti_{45.2}$ alloys respectively. In order to evaluate $Ni_{54.8}Ti_{45.2}$ transition temperatures, the alloy has been subjected to a thermal cycle: cooling from room temperature down to −30 °C and then heating up to 210 °C. Heat-flow curve is characterized by an endothermic transition during heating due to the formation of Austenite phase, defined by a start temperature (A_s = 43.7 °C) and a finish temperature (A_f = 64.7 °C). During the cooling, two exothermic transitions are present corresponding to Austenite → R-phase and R-phase → Martensite transitions, defined respectively by a R-phase start transition temperature (R_s = 51.0 °C) and a R-phase finish transition temperature (R_f = 33.8 °C) (Table 1). For each transition it is also possible to define a peak temperature, corresponding to the maximum temperature reached during the phase transformation and identified by the subscript "p" in Table 1. In order to verify alloy's transition temperatures, the sample has been subjected to further heating cycle up to 210 °C. A down shift of Austenite transition peak, A_p from 64.4 °C down to 58.4 °C has been found during this second cycle, confirmed by further heating–cooling cycles. Start and finish transition temperatures of $Ni_{55.4}Ti_{44.6}$ alloy have been evaluated from heat-flow curve and summarized in Table 1.

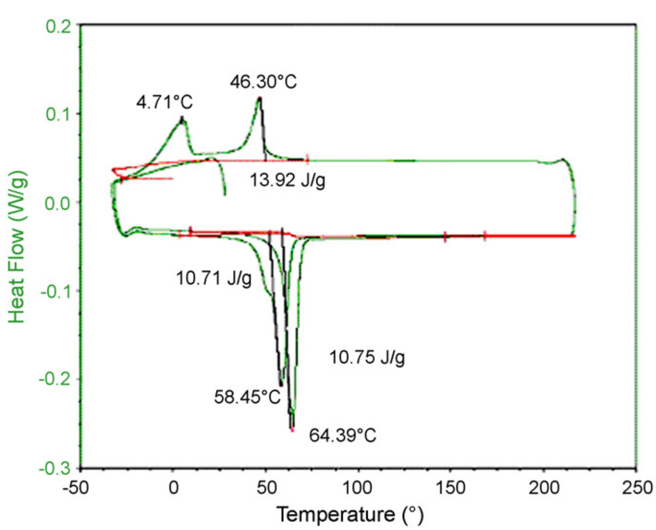

Fig. 1. $Ni_{55.4}Ti_{44.6}$ heat flow vs. temperature curve.

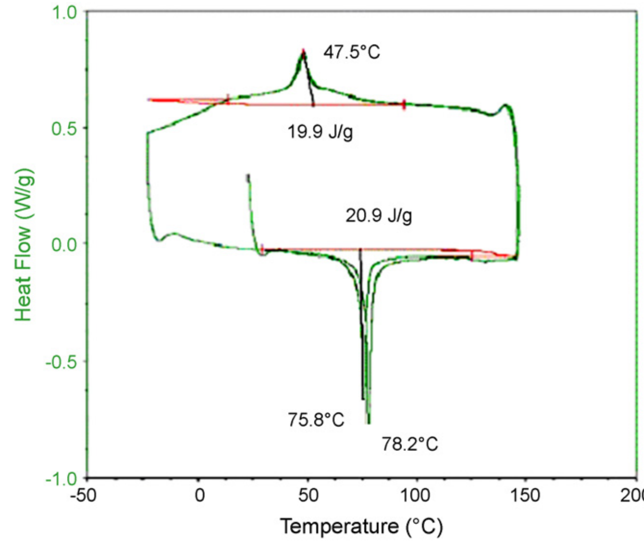

Fig. 2. $Ni_{54.8}Ti_{45.2}$ heat flow vs. temperature curve.

In order to evaluate $Ni_{54.8}Ti_{45.2}$ transition temperatures, the sample has been heated from environmental temperature up to 150 °C and then cooled down to −30 °C. During the heating, heat-flow curve is characterized by an endothermic transition due to the formation of Austenite phase defined by an Austenite start temperature (A_s = 66.7 °C) and an Austenite finish temperature (A_f = 85.0 °C). The cooling curve is characterized by

Table 1
$Ni_{55.4}Ti_{44.6}$ transition temperatures evaluated from DSC data

Martensite → Austenite	
A_s	43.6 °C
A_p	58.4 °C
A_f	64.7 °C
Austenite → R-phase	
R_s	51.0 °C
R_p	46.3 °C
R_f	33.8 °C
R-phase → Martensite	
M_s	9.78 °C
M_p	4.71 °C
M_f	−12.8 °C

Table 2
$Ni_{54.8}Ti_{45.2}$ transition temperatures evaluated from DSC data

Martensite → Austenite	
A_s	66.7 °C
A_p	75.8 °C
A_f	85.0 °C
Austenite → Martensite	
M_s	72.7 °C
M_p	47.5 °C
M_f	31.1 °C

the presence of a single exothermic transition due to the formation of Martensite from Austenite, defined by a Martensite start temperature (M_s = 72.7) and a Martensite finish temperature (M_f = 31.1 °C). The confirmation of transition temperatures has been carried out by increasing the temperature after the last cooling. As for the other alloy, this material exhibits a down shift of Austenite transition peak from 78.2 °C to 75.8 °C (A_p) (Table 2). Table 2 summarizes all transition temperature for $Ni_{54.8}Ti_{45.2}$ alloy.

2.2. *Electrical resistance measurements*

Electrical resistance (ER) measurements have been carried out using a home made four probes set-up. This electrical configuration is useful to remove contact resistances influence between NiTi sample and probes. A current generator has been built as supplier for the electrical system, with a current of 478 μA ± 0.1% and a temperature sensitivity of 10 ppm/°C. This current circulating in the wire influenced SMA wires temperature less than 0.1 °C, which was the accuracy of all temperature measurements. Because of the very low NiTi wires resistance, a low noise signal amplifier has been built (supply = +9 V to 9 V referred to the ground; gain factor = 1025 ± 2%; bandwidth = 25 kHz) in order to amplify voltage values acquired. All measurements were acquired using National Instruments DAQ-PAD 6052E and Labview.

In order to study temperature dependence of NiTi resistivity, all samples have been heated and cooled in a thermostatic chamber at a constant rate of 10 °C/min and 2 °C/min respectively and using liquid nitrogen for temperature below 25 °C. Fig. 3 shows a schematic of the electrical resistivity measurements set-up.

Electrical resistivity ρ of a wire of length L and cross-sectional area A has been evaluated as

$$\rho = \frac{V}{I}\frac{A}{L} \quad (1)$$

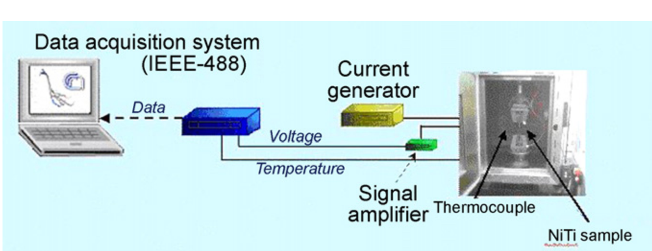

Fig. 3. Electrical resistivity measurements experimental set-up.

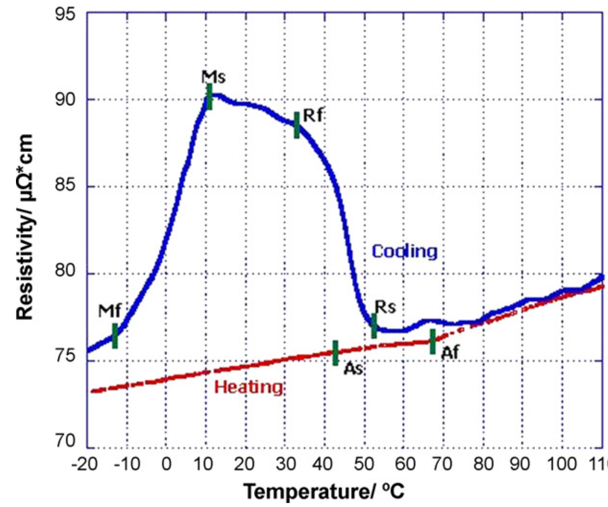

Fig. 4. Electrical resistivity vs. temperature diagram of $Ni_{55.4}Ti_{44.6}$ alloy.

where I is the current value and V is the voltage value measured during the thermal cycles.

3. Experimental results and discussion

3.1. *$Ni_{55.4}Ti_{44.6}$ alloy*

$Ni_{55.4}Ti_{44.6}$ electrical resistivity has been measured in the temperature range −20 °C to 110 °C. Fig. 4 shows the resistivity versus temperature diagram for heating and cooling.

A typical NiTi resistivity curve during heating was found, pointing out the transformation from Martensite to Austenite. Resistivity measurements started from −20 °C, below Martensite finish temperature (around −10 °C), and hence no trace of R-phase is present in the sample. Temperature variation of electrical resistivity in this first heating is linear and only two slight slope changes are present in correspondence of Austenite start and finish temperatures. During the cooling, resistivity curve is characterized by a “cap” due to the presence of R-phase in the transition Austenite → R-phase → Martensite and defined at higher temperatures by R_s and R_f and at lower temperatures by M_f and M_s [2,3,7]. Transition temperatures are evidenced in Fig. 4 and summarized in Table 3. These values are quite similar to temperature values obtained from calorimetric test with differences less than 2 °C.

Table 3
$Ni_{5.4}Ti_{44.6}$ transition temperatures evaluated from resistivity data

Martensite → Austenite	
A_s	42.8 °C
A_f	66.3 °C
Austenite → R-phase	
R_s	52.5 °C
R_f	33.4 °C
R-phase → Martensite	
M_s	10.7 °C
M_f	−11.6 °C

The availability of calorimetric and resistivity data allowed the evaluation of the converted fraction of each phase as function of temperature. For DSC data converted fractions of each phase as a function of temperature have been calculated as the ratio between the current and the total area evaluated from DSC heat-flow curve. Using this method, Martensite and R-phase converted fractions have been evaluated by exothermic peaks found during the cooling and Austenite converted fraction by the endothermic peak evidenced during the heating cycle.

Converted fractions of each phase have been evaluated also using resistivity results, where resistivity is a function of the temperature. In order to get an expression of converted phase as a function of $\rho(T)$, the mixing rule has been used, where the total resistivity has been considered as the sum of resistivity of each phase. This assumption is based on literature studies, reporting that thermodynamical properties of SMA and thermally induced martensitic transformations can be modeled by using the mixing rule [17]. Moreover, the comparison between converted fractions derived from DSC data and those derived from electrical measurements provided a good agreement between results.

In order to find an expression of the converted percentage for each phase, at first experimental resistivity data have been linearly interpolated in the temperature ranges where a single phase exists. Then, on the basis of the mixing rule for the resistivity, the following relationships for the phase fractions x have been considered:

$$x_{\mathrm{m}} = \frac{\rho(T) - \rho_{\mathrm{a}}(T)}{\rho_{\mathrm{m}}(T) - \rho_{\mathrm{a}}(T)} \text{ transition (M} \rightarrow \text{A) during heating,}$$
$$x_{\mathrm{m}} = \frac{\rho(T) - \rho_{\mathrm{r}}(T)}{\rho_{\mathrm{m}}(T) - \rho_{\mathrm{r}}(T)} \text{ transition (R} \rightarrow \text{M) during cooling,}$$
$$x_{\mathrm{r}} = \frac{\rho(T) - \rho_{\mathrm{a}}(T)}{\rho_{\mathrm{r}}(T) - \rho_{\mathrm{a}}(T)} \text{ transition (A} \rightarrow \text{R) during cooling} \quad (2)$$

where ρ is the experimental resistivity, the suffices a, m, r are relative to Austenite, Martensite and R-phase, respectively.

The first equation in (2) expresses the Martensite fraction decreasing during heating passing from one at a temperature lower than A_s to 0 at a temperature higher than A_f. The other two equations express respectively the Martensite fraction increasing from 0 to 1, during cooling from R-phase and the R-phase fraction increasing from 0 to 1, during cooling from Austenite phase.

Fig. 5 shows the comparison between phase fractions evaluated from DSC data and the same phase fractions evaluated using resistivity data during the transformation from Martensite to Austenite. Fig. 6(a) and (b) shows phase fractions of R-phase and Martensite respectively evaluated both using DSC and ER data for the two-stage transformation Austenite → R-phase → Martensite. From the comparison between converted fractions evaluated from DSC and resistivity data, a good agreement was found in all temperature ranges, confirming the reliability and the capability of electrical resistivity measurements to quantify phase transformation fractions.

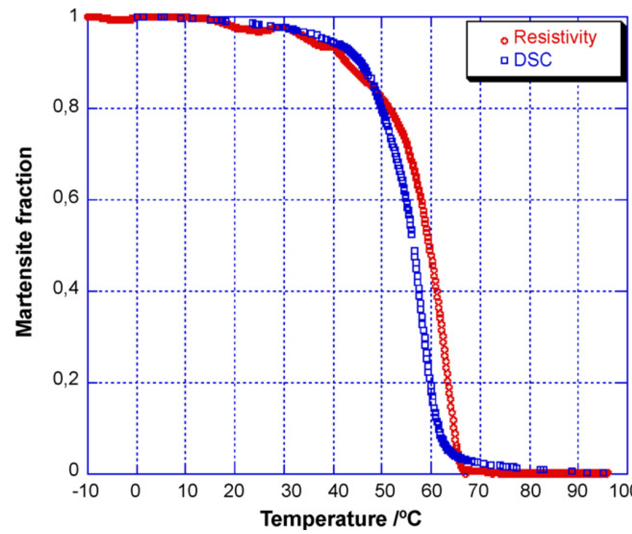

Fig. 5. Comparison between phase fractions evaluated from DSC data and ER measurements during Martensite → Austenite transformation for $Ni_{55.4}Ti_{44.6}$ alloy.

3.2. $Ni_{54.8}Ti_{45.2}$ alloy

$Ni_{54.8}Ti_{45.2}$ alloy has been electrically characterized in the temperature range 30–140 °C. Fig. 7 shows alloy's electrical resistivity versus temperature graph, measured during a heating cycle from 35 °C to 140 °C and a cooling cycle from 140 °C to 35 °C. During the heating, a drop was found, denoting the transition from a mixed phase consisting of R-phase and Martensite (M + R) to Austenite. This is due to the fact that R-phase is characterized by the higher resistivity value among the tree NiTi crystallographic phases. For the same reason, during the cooling an increase of resistivity was found because of the transition from Austenite to R-phase.

It is important to outline that R-phase was not detectable from heat-flow curve (Fig. 2) that was characterized by one endothermic peak for Martensite → Austenite transition and one exothermic peak for Austenite → Martensite transition. From the analysis of resistivity diagram transition temperatures can be determined (Table 4).

Phase fractions have been evaluated both from DSC heat-flow curve and resistivity data using the same procedure used for the first alloy. M + R fraction has been evaluated from resistivity

Table 4
$Ni_{54.8}Ti_{45.2}$ transition temperatures evaluated from resistivity data

Martensite → Austenite	
A_s	68.6 °C
A_f	92.7 °C
Austenite → R-phase	
R_s	77.8 °C
R_f	52.2 °C
R-phase → Martensite	
M_s	47.7 °C
M_f	–

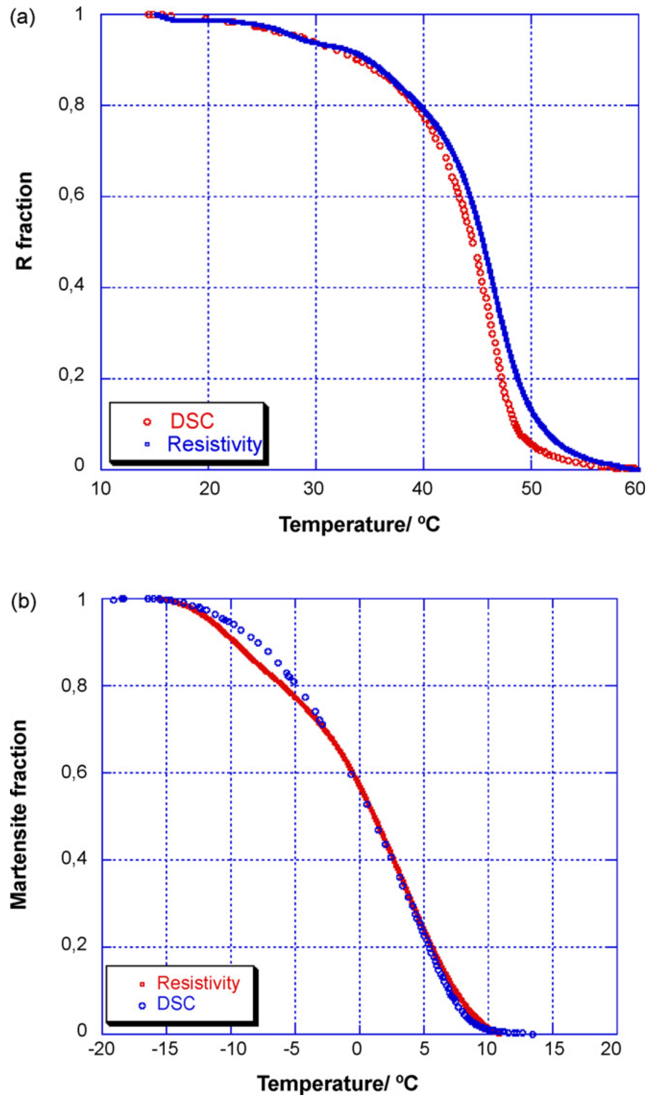

Fig. 6. Comparison between phase fractions evaluated from DSC data and ER measurements during a) Austenite → R-Phase and b) R-Phase → Martensite transformations for $Ni_{55.4}Ti_{44.6}$ alloy.

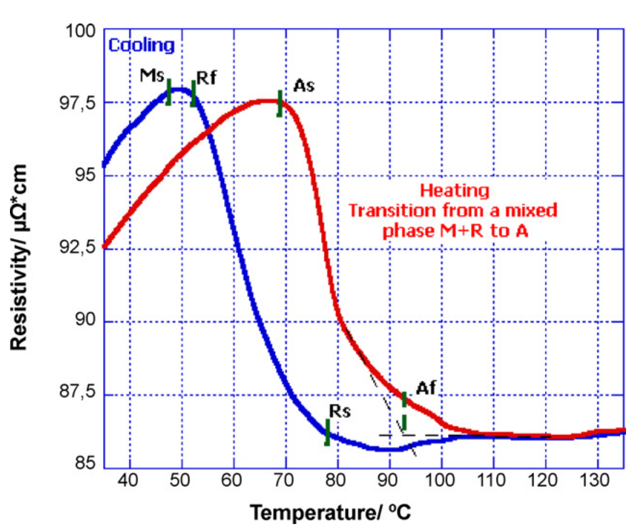

Fig. 7. Electrical resistivity vs. temperature diagram of $Ni_{54.8}Ti_{45.2}$ alloy.

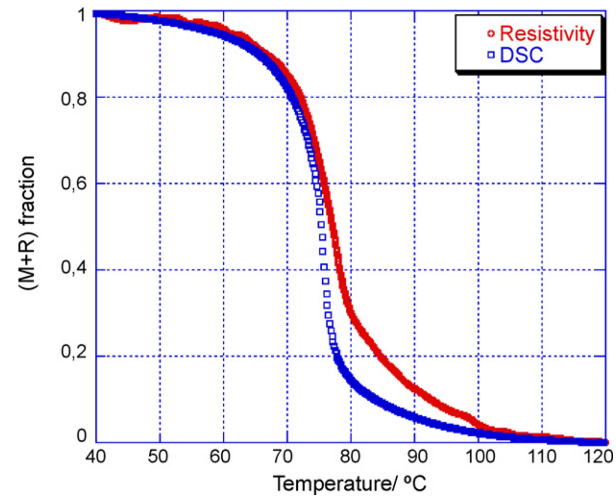

Fig. 8. Comparison between phase fractions evaluated from DSC data and ER measurements during R-Phase-Martensite → Austenite transformation for $Ni_{54.8}Ti_{45.2}$ alloy.

measurements during cooling from Austenite as

$$x_{m+r} = \frac{\rho(T) - \rho_a(T)}{\rho_{m+r}(T) - \rho_a(T)} \text{ transition (A} \rightarrow \text{M+R) during cooling} \quad (3)$$

Figs. 8 and 9 report the comparison between R-phase–Martensite mixed phase fraction obtained by DSC and resistivity data upon heating and cooling cycles.

As expected, due to different A_f values deriving from DSC and ER measurements, a slight difference between M + R fractions DSC and ER graphs is observed, in particular during heating in the Austenite formation region (Fig. 8). On the contrary, during cooling in correspondence of the reverse transformation from Austenite to M + R-phase (Fig. 9) a good agreement between DSC and resistivity data was found. In addition, the knowledge of R_s, R_f and M_s temperatures by ER results allows to the explicit identification of Austenite → R-phase and

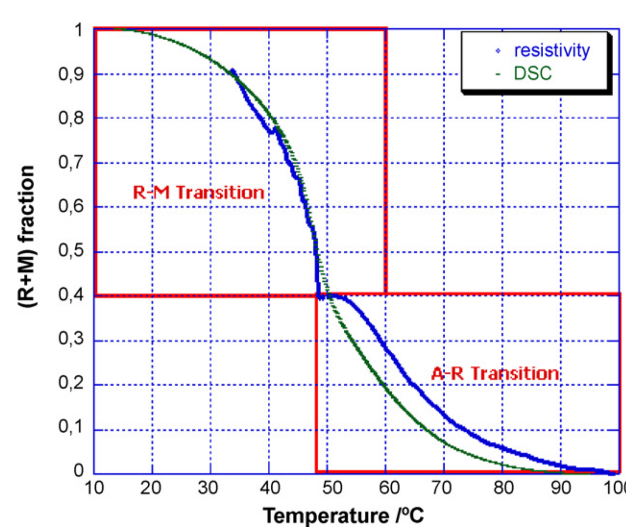

Fig. 9. Comparison between phase fractions evaluated from DSC data and ER measurements during Austenite → R-Phase-Martensite transformation for $Ni_{54.8}Ti_{45.2}$ alloy.

R-phase → Martensite transitions. In particular, it is possible to observe that the Martensite formation occurs when about the 60% of Austenite is already converted into R-phase.

4. Conclusion

Two Nitinol alloys' ($Ni_{55.4}Ti_{44.6}$ and $Ni_{54.8}Ti_{45.2}$) transformation behavior has been investigated by calorimetric analysis and electrical resistance measurements, in order to evaluate transition temperatures and phase transformation degree during heating and cooling. A comparison between these two characterization techniques has been carried out, providing a good agreement between calorimetric and electrical results and the quantification of transformation phase degree. ER measurement has proved to be a good probe for the identification of various phases in SMA, resulting more sensitive than conventional DSC technique in the evaluation of R-phase and of its start and finish transition temperatures. Moreover, for $Ni_{54.8}Ti_{45.2}$ the presence of a mixed phase constituted by Martensite and R-phase has been detected from ER measurements but not from DSC analysis, where only a large peak transition in the cooling part of heat-flow curve is present. ER measurements clearly revealed the presence of R-phase both during heating and cooling, being R-phase resistance higher than Austenite and Martensite ones.

References

[1] M. Cohen, Trans. Jpn. Inst. Met. 29 (8) (1988) 609.
[2] J. Uchil, K.P. Mohanachandra, K. Gesh Kumara, K.K. Mahesh, Mater. Sci. Eng. A 251 (1998) 58–63.
[3] J. Uchil, K. Ganesh Kumara, K.K. Mahesh, Mater. Sci. Eng. A 332 (1–2) (2002) 25.
[4] H. Matsumoto, J. Mater. Sci. Lett. 11 (1992) 367.
[5] H. Matsumoto, J. Mater. Sci. Lett. 8 (1989) 1783.
[6] C.Y. Xie, L.C. Zhao, T.C. Lei, Scripta Metall. 23 (1989) 2131.
[7] J. Uchil, K.K. Mahesh, K. Ganesh Kumara, Physica B 324 (2002) 419–428.
[8] M. Pozzi, G. Airoldi, Mater. Sci. Eng. A273–275 (1999) 300–304.
[9] X.D. Wu, Y.Z. Fan, J.S. Wu, Mater. Des. 21 (2000) 511–515.
[10] M.G. Faulkner, J.J. Amalraj, A. Bhattacharyya, Smart Mater. Struct. 9 (2000) 632–639.
[11] G. Airoldi, G. Riva, B. Rivolta, M. Vanelli, J. Therm. Anal. 42 (1994) 781.
[12] Z.C. Lin, P.C.W. Fung, J.X. Zhang, K.F. Liang, Solid State Commun. 75 (5) (1990) 390.
[13] D. Stronz, Z. Bojarski, J. Ilczuk, Z. Lekston, H. Morawiec, J. Mater. Sci. 26 (1991) 1741.
[14] T. Todoroki, H. Tamura, Trans. Jpn. Inst. Met. 28 (2) (1987) 83–84.
[15] G.V. Lashkarev, S.M. Solonin, A.V. Brodovoi, I.F. Martynova, M.V. Radchenko, A.L. Mirets, N.V. Goncharuk, Sov. Phys. Solid State 34 (2) (1992) 352.
[16] X. Wu, J. Wu, Z. Weng, Sand Struct. 8 (1999) 575–578.
[17] Y. Huo, X. Zu, Continuum Mech. Therm. 10 (3) (1998) 179–188.